Spec. Publs int. Ass. Sediment. (1986) **8**, 327–345

Evolution from passive margin to foreland basin: the Atoka Formation of the Arkoma Basin, south-central U.S.A.

DAVID W. HOUSEKNECHT

Department of Geology, University of Missouri, Columbia, Missouri 65211, U.S.A.

ABSTRACT

Atokan strata of the Arkoma basin record the transition from sedimentation on a passive, rifted margin to sedimentation in a foreland basin developed by convergent tectonic activity along the Ouachita orogenic belt. The basal Atoka Spiro sandstone was deposited along a tidally swept coastline on a tectonically stable shelf that had prevailed since the late Cambrian. The remainder of the Atoka Formation was deposited during the breakdown of that shelfal area by normal faults, apparently induced by obduction of the Ouachita accretionary prism on to the southern margin of North American crust. The resulting wedge of Atokan strata displays evidence of syndepositional fault movement that significantly influenced sediment dispersal patterns, distribution of certain facies, and thickness patterns within the basin. Deposition on a muddy slope dissected by tectonically localized slope channels characterized that part of the basin where active fault movement was occurring. By the end of Atokan time, syndepositional faulting had ceased, and flexural subsidence and deposition of coal-bearing molasse characterized the final phase of foreland basin evolution.

INTRODUCTION

Strata of the Arkoma basin and Ouachita orogenic belt reflect the opening and subsequent closing of a Palaeozoic ocean basin (Iapetus). Carboniferous strata of the region were deposited during the final phase of ocean basin closing, and record the transition from sedimentation on a passive, rifted margin to synorogenic sedimentation in a rapidly evolving foreland basin. The objectives of this paper are to review the Palaeozoic tectonic history of the southern margin of North America culminating with the Ouachita orogenic event, to document geometric characteristics of the foreland basin that formed as a consequence of that orogenic event, and to present an overview of the Pennsylvanian depositional history of the basin with emphasis on the active influence exerted by tectonic activity.

GEOLOGICAL SETTING

The Arkoma is one of a series of foreland basins that formed along the North American side of the Ouachita orogenic belt during the Carboniferous. The Ouachita Mountains, extending from central Arkansas into south-eastern Oklahoma (Fig. 1), represent the largest exposure of this orogenic belt that lies mostly buried beneath Mesozoic and Cenozoic strata of the Gulf coastal plain. The foreland region along the entire length of the Ouachita orogenic belt generally shared a common history of rifted margin sedimentation during the early to middle Palaeozoic followed by foreland basin development induced by convergent tectonism during the late Palaeozoic (Flawn *et al.*, 1961; Graham, Dickinson & Ingersoll, 1975; Thomas, 1985). Only during the final phases of Ouachita orogenesis was the foreland region segmented into individual structural basins, one of which is the Arkoma.

The Arkoma basin is an accurate synclinorium that extends from east-central Arkansas to south-eastern Oklahoma (Fig. 1). It lies immediately north of the Ouachita orogenic belt, to which it is intimately related. Although the southern margin of the basin is historically defined as the northern edge of the Ouachita frontal thrust belt, it is now clear that Atokan strata exposed in the frontal thrust belt were

Foreland Basins Edited by P. A. Allen and P. Homewood

 ISBN: 978-0-632-01732-4

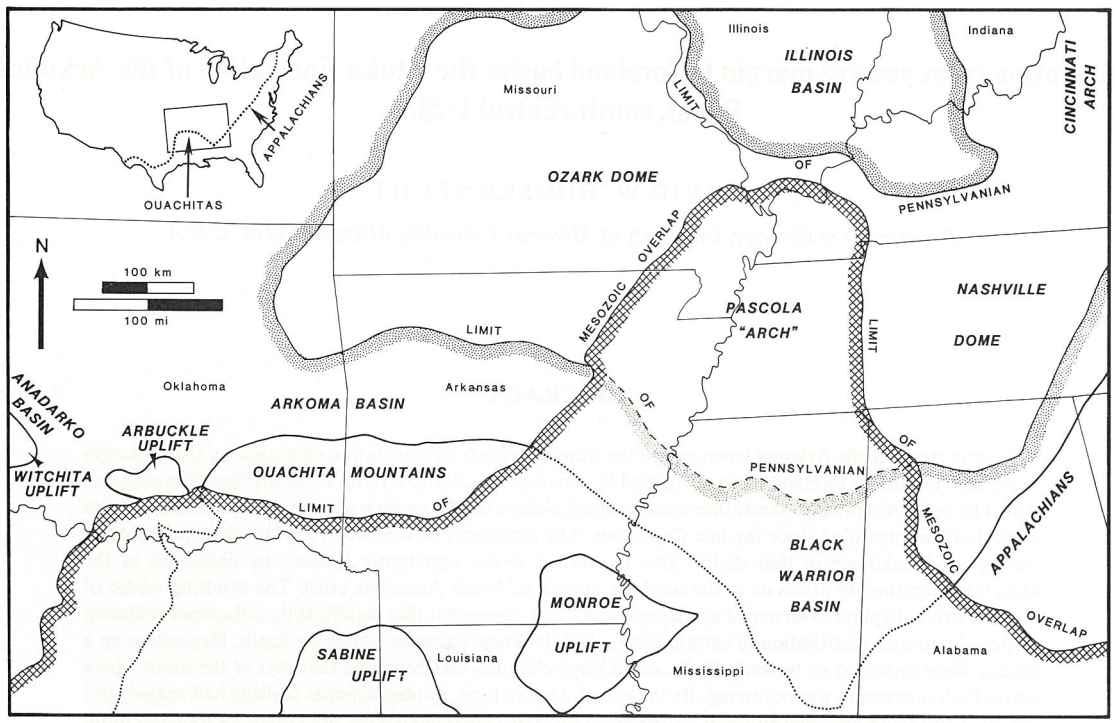

Fig. 1. Regional map showing geological setting of Arkoma basin.

deposited in continuity with Arkoma basin strata and that older Arkoma basin strata extend southwards for an unknown distance beneath the thrust belt.

Figure 2 schematically summarizes the Palaeozoic stratigraphy of the Arkoma basin and Ouachita Mountains. Upper Cambrian to basal Atokan strata within the basin comprise shallow marine carbonates, shales, and quartzose sandstones whose maximum aggregate thickness along the southern part of the basin is about 1·5 km. Because of their peripheral importance to this paper, they are grouped as 'undifferentiated, rifted-margin shelf strata' in Fig. 2. The overlying Atoka Formation comprises shales and sandstones that display complex stratigraphic and facies characteristics that are detailed in the following text. Deposited during a mere 5 Myr interval of time, the Atoka attains a maximum thickness of more than 5·5 km along the southern margin of the basin. Conformably overlying the Atoka are coal-bearing formations of Desmoinesian age that attain a maximum aggregate thickness of about 2·5 km. The Ouachita stratigraphic section is readily divisible into two parts. The lower part includes Ordovician to lowermost Mississippian strata that probably attain a maximum thickness of about 3·7 km. These strata are predominantly deep marine shales with subordinate beds of limestone, quartzose sandstone, and bedded chert. Because of their peripheral importance to this paper, they are grouped as 'undifferentiated, rifted-margin, deep basin strata' in Fig. 2. Mississippian to middle Atokan strata of the Ouachitas comprise shales and sandstones (Stanley, Jackfork, Johns Valley, and Atoka Formations of Fig. 2) whose aggregate thickness exceeds 10 km. These Carboniferous strata constitute a flysch sequence whose deposition on submarine fans and in associated deep water environments is well documented (e.g. Morris, 1974; Moiola & Shanmugam, 1984).

Within the Arkoma basin, broad synclines separated by narrow anticlines dominate the structure at the surface (Fig. 3). The axes of these folds generally parallel the overall arcuate trend of the basin and that of the Ouachita frontal thrust belt. Listric thrust faults are known to underlie much of the folded section and ramp to the surface along the crests of many anticlines (Fig. 3). Beneath thrust fault horizons, the structural style is dominated by normal faults that offset Precambrian basement and the entire sub-Atoka

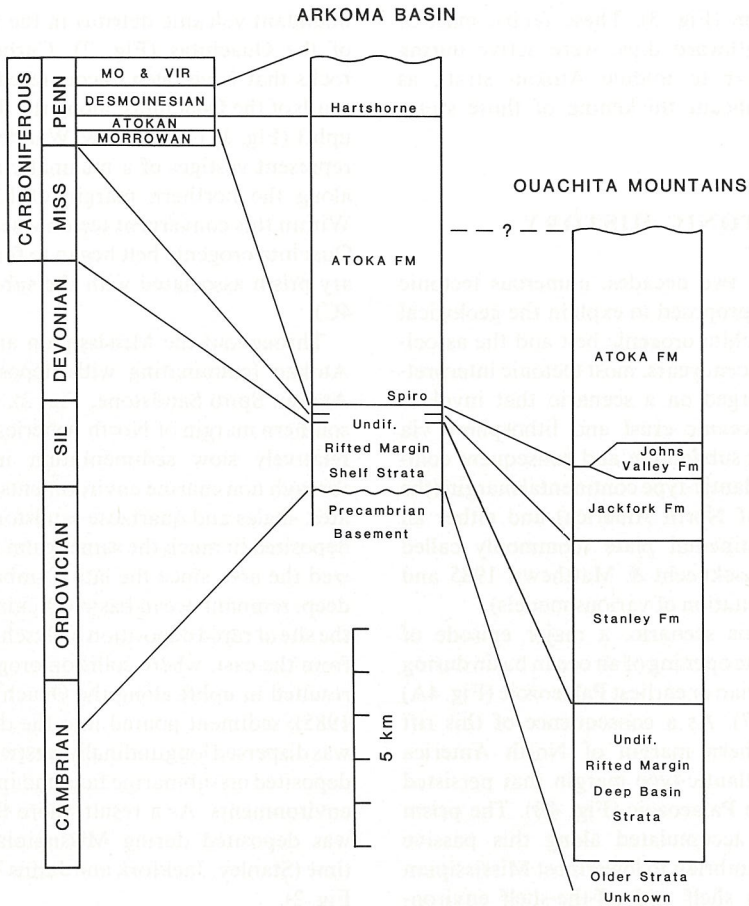

Fig. 2. Generalized stratigraphic columns of Arkoma basin and Ouachita Mountains. Wavy lines at top of columns represent present erosion surface.

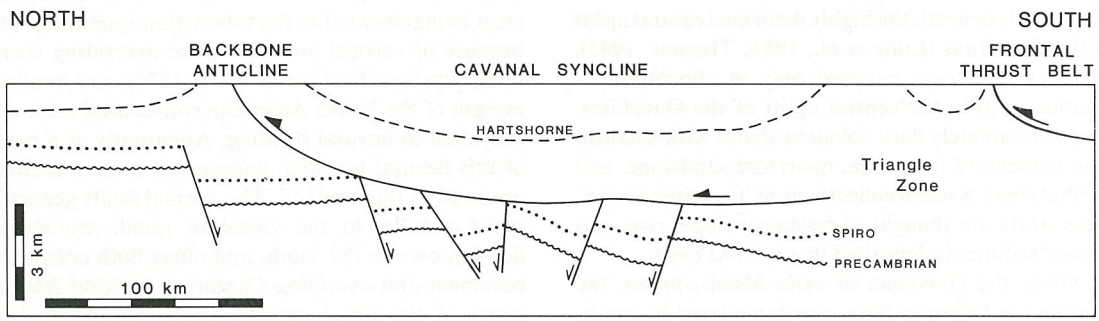

Fig. 3. Generalized tracing of a seismic line extending from north of Backbone anticline southward to Ouachita frontal thrust belt (see Fig. 5), illustrating the structural style of the Arkoma basin. Wavy line is approximate Precambrian–Cambrian unconformity; dotted line is approximate horizon of basal Atoka Spiro sandstone; dashed line is approximate horizon of basal Desmoinesian Hartshorne Sandstone and heavy solid lines are faults, with displacements indicated by arrows. Upper parts of syndepositional normal faults are displaced northwards by thrust fault, but are not shown on this figure.

sedimentary section (Fig. 3). These faults, most of which display southward dips, were active during deposition of lower to middle Atokan strata as indicated by significant thickening of those strata across the faults.

TECTONIC HISTORY

During the past two decades, numerous tectonic models have been proposed to explain the geological history of the Ouachita orogenic belt and the associated foreland. In recent years, most tectonic interpretations have converged on a scenario that involves consumption of oceanic crust and lithosphere via southward-dipping subduction and consequent collision between an Atlantic-type continental margin (the southern margin of North America) and either an island arc or continental plate (commonly called Llanoria) (see Houseknecht & Matthews, 1985 and Thomas, 1985 for citation of various models).

According to this scenario, a major episode of rifting resulted in the opening of an ocean basin during the latest Precambrian or earliest Palaeozoic (Fig. 4A) (e.g. Thomas, 1977). As a consequence of this rift opening, the southern margin of North America evolved into an Atlantic-type margin that persisted through the middle Palaeozoic (Fig. 4B). The prism of sediment that accumulated along this passive margin includes Cambrian to lowermost Mississipian strata deposited in shelf and off-the-shelf environments. Shelf facies are predominately carbonates with subordinate volumes of shale and quartzose sandstone. Although their original southward extent is unknown, they are present throughout the Arkoma basin and the lower Palaeozoic portion is believed to extend southwards beneath the highly deformed central uplift of the Ouachitas (Lillie *et al.*, 1983; Thomas, 1985). Off-the-shelf facies, exposed only in allochthonous positions within the central uplift of the Ouachitas, are predominately dark coloured shales with subordinate volumes of limestone, quartzose sandstone, and bedded chert. Known collectively as 'Ouachita facies', these strata are thought to represent slope, rise, and abyssal sediments deposited in a starved basin.

During the Devonian or early Mississippian, the ocean basin began to close, accommodated by southwards subduction beneath Llanoria (Fig. 4C). Although it is impossible to determine precisely when subduction began, it was clearly under way during the Mississippian, as suggested by detritus indicative of an orogenic provenance (Morris, 1974) and locally abundant volcanic detritus in the Stanley Formation of the Ouachitas (Fig. 2). Carboniferous volcanic rocks that have been encountered in the subsurface south of the Ouachitas, along the flanks of the Sabine uplift (Fig. 1) (Nicholas & Waddell, 1982), probably represent vestiges of a magmatic arc that developed along the northern margin of Llanoria (Fig. 4C). Within this convergent tectonic setting, the incipient Ouachita orogenic belt began to form as an accretionary prism associated with the subduction zone (Fig. 4C).

Throughout the Mississipian and into the earliest Atokan (culminating with deposition of the basal Atokan Spiro Sandstone, Fig. 2), the shelf along the southern margin of North America remained a site of relatively slow sedimentation in shallow marine through non-marine environments (Fig. 4C). Carbonates, shales and quartzose sandstones continued to be deposited in much the same realm that had characterized the area since the late Cambrian. However, the deep, remnant ocean basin (Dickinson, 1974) became the site of rapid deposition of flysch. Derived primarily from the east, where collision orogenesis had already resulted in uplift along the Ouachita trend (Thomas, 1985), sediment poured into the deep basin where it was dispersed longitudinally westwards and ultimately deposited on submarine fans and in associated abyssal environments. As a result, more than 5 km of flysch was deposited during Mississipian and Morrowan time (Stanley, Jackfork and Johns Valley Formations, Fig. 2).

By early Atokan time, the remnant ocean basin had been consumed by subduction and the northward advancing subduction complex was being obducted on to the rifted continental margin of North America (Fig. 4D). Partly as a result of attenuated continental crust being drawn into the subduction zone and partly because of vertical loading by the overriding accretionary prism (Dickinson, 1974, 1976), the southern margin of the North American continental crust was subjected to flexural bending. Apparently as a result of this flexural bending, widespread normal faulting occurred in the foreland. The normal faults generally strike parallel to the Ouachita trend, are mostly downthrown to the south, and offset both crystalline basement and overlying Cambrian to basal Atokan strata of the rifted margin prism. Subsurface and seismic evidence suggests that most of these faults broke previously undeformed continental crust, although it is likely that some of them may represent reactivation of faults formed during early Palaeozoic rifting (Fig. 4). The shelf-slope-rise geometry that had

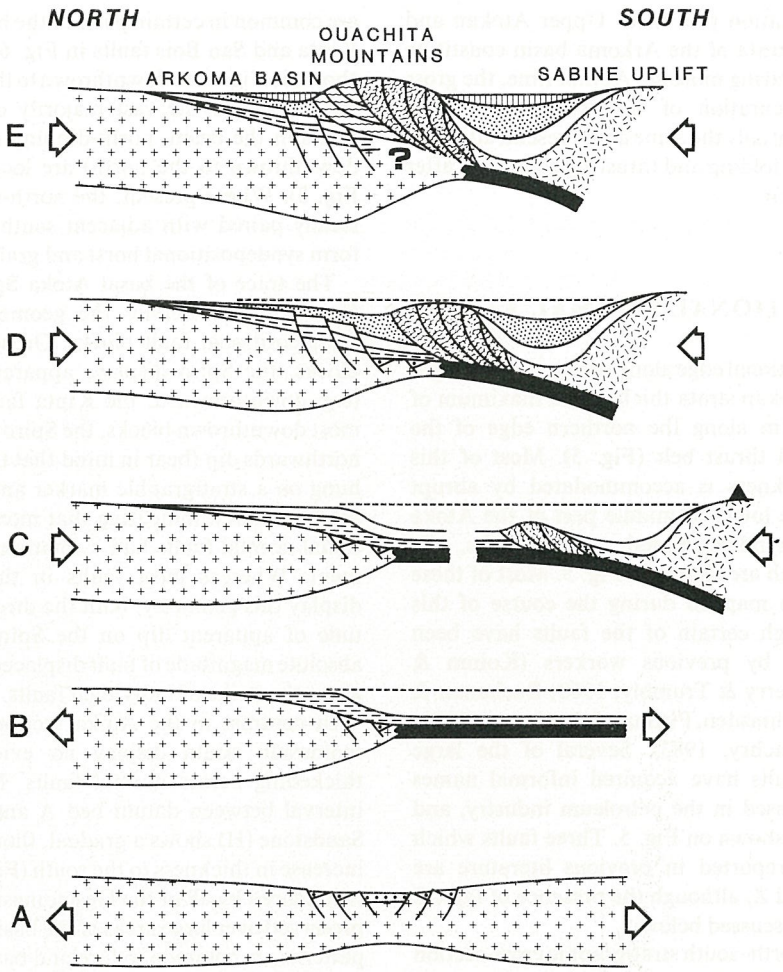

Fig. 4. Hypothetical cross-sections depicting tectonic evolution of southern margin of North America during (A) late Precambrian–earliest Palaeozoic, (B) late Cambrian–earliest Mississippian, (C) early Mississippian–earliest Atokan, (D) early–middle Atokan, and (E) late Atokan–Desmoinesian. Key to patterns: crosses = continental crust (undifferentiated in A, North American in B–E); straw hachures = 'Llanorian' crust; black = oceanic crust; heavy dots = basal Palaeozoic strata; horizontal hachures = upper Cambrian–basal Mississippian strata; white = Mississippian–basal Atokan strata; sand stippling = lower–middle Atoka strata; vertical lines = upper Atokan–Desmoinesian strata; mottled = Ouachita subduction complex; wavy lines = Ouachita foreland thrust belt; black trinagle = magmatic arc volcanoes. Figure modified from Houseknecht & Matthews (1985).

prevailed along the passive continental margin since the early Palaeozoic was broken down by the tectonically induced normal faults and rates of both subsidence and sedimentation increased markedly. Fault movement was contemporaneous with deposition of lower to middle Atokan shales and sandstones, resulting in abrupt thickness increases across faults (Fig. 4D). These Atokan strata represent a critical transition between passive margin sedimentation and foreland basin sedimentation, and are the topic of most of the following discussion.

By late Atokan time (Fig. 4E), foreland-style thrusting became predominant as the subduction complex pushed northwards against strata deposited in settings illustrated by Fig. 4 (C, D). Resultant uplift along the frontal thrust belt of the Ouachitas completed the formation of a peripheral foreland basin (Dickinson, 1974) in which shallow marine, deltaic, and

fluvial sedimentation prevailed. Upper Atokan and Desmoinesian strata of the Arkoma basin constitute a typical coal-bearing molasse. At that time, the gross structural configuration of the Arkoma–Ouachita system was essentially the same as at present, although relatively minor folding and thrusting continued after the Desmoinesian.

SYNDEPOSITIONAL NORMAL FAULTS

From a depositional edge along the northern margin of the basin, Atokan strata thicken to a maximum of more than 5·5 km along the northern edge of the Ouachita frontal thrust belt (Fig. 5). Most of this increase in thickness is accommodated by abrupt expansion of the lower to middle part of the Atoka section across syndepositional normal faults, the locations of which are shown in Fig. 5. Most of these faults have been mapped during the course of this research, although certain of the faults have been mapped locally by previous workers (Koinm & Dickey, 1967; Berry & Trumbly, 1968; Buchanan & Johnson, 1968; Lumsden, Pittman & Buchanan, 1971; Haley, 1982; Zachry, 1983). Several of the large displacement faults have acquired informal names that are widely used in the petroleum industry, and those names are shown on Fig. 5. Three faults which have not been reported in previous literature are labelled X, Y and Z, although the presence of fault Z is equivocal as discussed below.

Figure 6 is a north–south stratigraphic cross-section whose datum (labelled A) is a widespread log-response anomaly in the upper part of the Atoka Formation and whose lower key bed is the basal Atoka Spiro sandstone (labelled S). Constructed from wire-line logs of 41 wells, cross-section A–A′ illustrates the fault-controlled geometry of Atokan strata in a part of the basin that is unaffected by thrust faults of large displacement (Fig. 5). Southwards along the line of section, the Atoka increases in thickness from 760 m to more than 3700 m, with most of the increase occurring in abrupt steps across a few faults with displacements of several hundred to more than 1000 m. Some of the large displacement faults appear to have a single plane of movement (e.g. Kinta fault) whereas others splay into two (San Bois fault) or more (Mulberry fault) discrete fault planes (Figs 5 and 6). In addition to those with large displacements, numerous syndepositional normal faults with smaller displacements (generally less than a few hundred metres) are common in certain parts of the basin (e.g. between Kinta and San Bois faults in Fig. 6). All of the faults shown in Fig. 6 are downthrown to the south. Although this is true of the vast majority of syndepositional faults in the basin, north-dipping normal faults (i.e. downthrown to the north) are locally common (see Fig. 3). Where present, the north-dipping faults are locally paired with adjacent south-dipping faults to form syndepositional horst and graben geometries.

The trace of the basal Atoka Spiro sandstone on Fig. 6 further defines the geometry of individual syndepositional fault blocks. On some downthrown blocks, the Spiro displays apparent southward dip (e.g. downthrown to the Kinta fault). However, on most downthrown blocks, the Spiro displays apparent northwards dip (bear in mind that the cross-section is hung on a stratigraphic marker and does not depict true structure), indicating that most of the sydepositional normal faults had a rotational sense of movement. Whereas most faults in the Arkoma basin display this geometry, both the direction and magnitude of apparent dip on the Spiro, as well as the absolute magnitude of fault displacement, are variable along the strike of individual faults.

In contrast to the Atoka section, overlying Desmoinesian strata display no evidence of abrupt thickening across normal faults. For example, the interval between datum bed A and the Hartshorne Sandstone (H) shows a gradual, though asymmetrical increase in thickness to the south (Fig. 6), a characteristic shared by all of the Desmoinesian strata that are preserved over large areas of the basin. Such thickness patterns are common to foreland basins and probably result from flexural subsidence induced by foreland-style thrust loading along margins of basins adjacent to orogenic belts (Jordan, 1981).

Figure 7 is a NW–SE cross-section constructed from wire-line logs of five wells. This section is located in a part of the basin that has been subjected to thrust faulting and is necessarily more schematic than Fig. 6 because of fewer data points. Nevertheless, it can be used to illustrate important aspects of syndepositional normal faulting and Atokan stratigraphy. Significantly, cross-section B–B′ extends southward into a deeper portion of the basin than cross-section A–A′. Notice that the San Bois fault is present near the south end of cross-section A–A′ and near the north end of cross-section B–B′. As an example of variable fault displacement along strike, there is over 3300 m of section between bed A and the Spiro downthrown to the San Bois fault in cross-section A–A′ (Fig. 6) whereas the same interval downthrown to the San

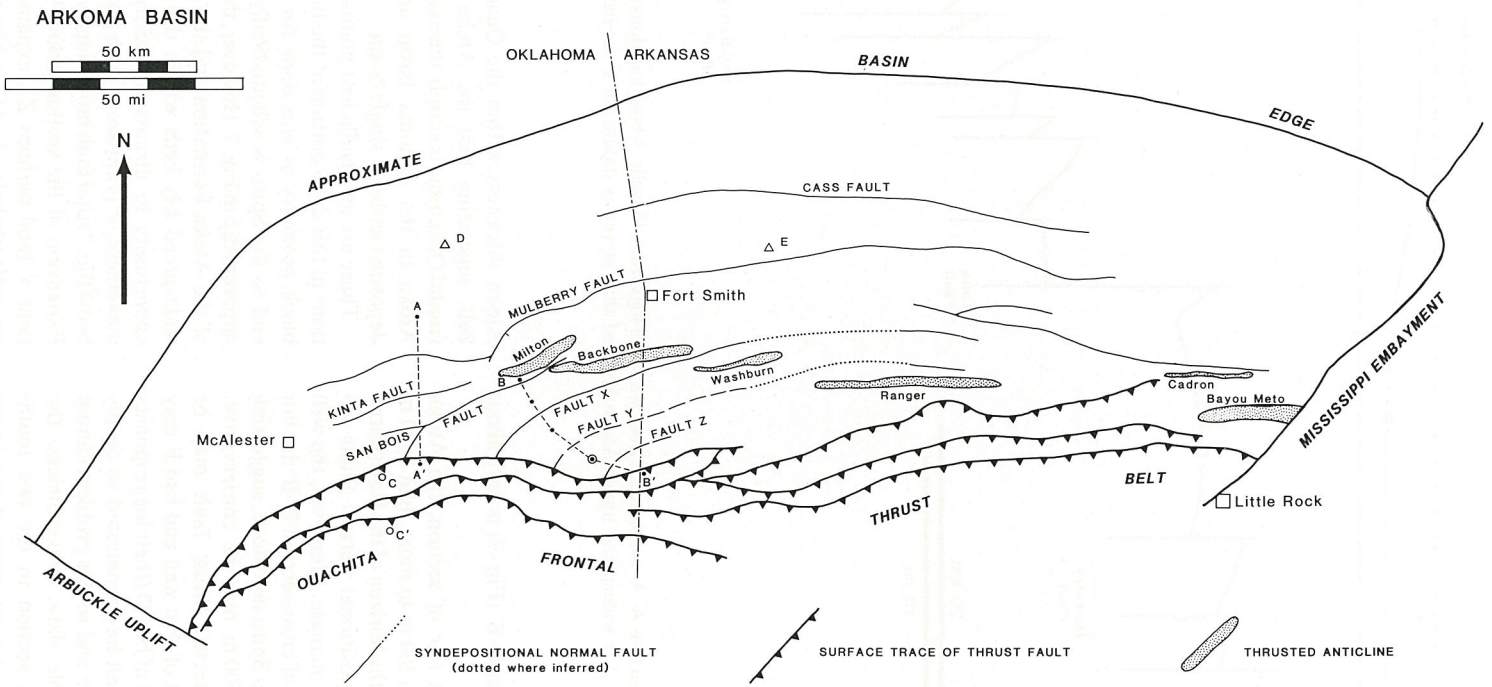

Fig. 5. Base map of Arkoma basin showing locations of known syndepositional normal faults, and lines of cross-section and other localities discussed in text.

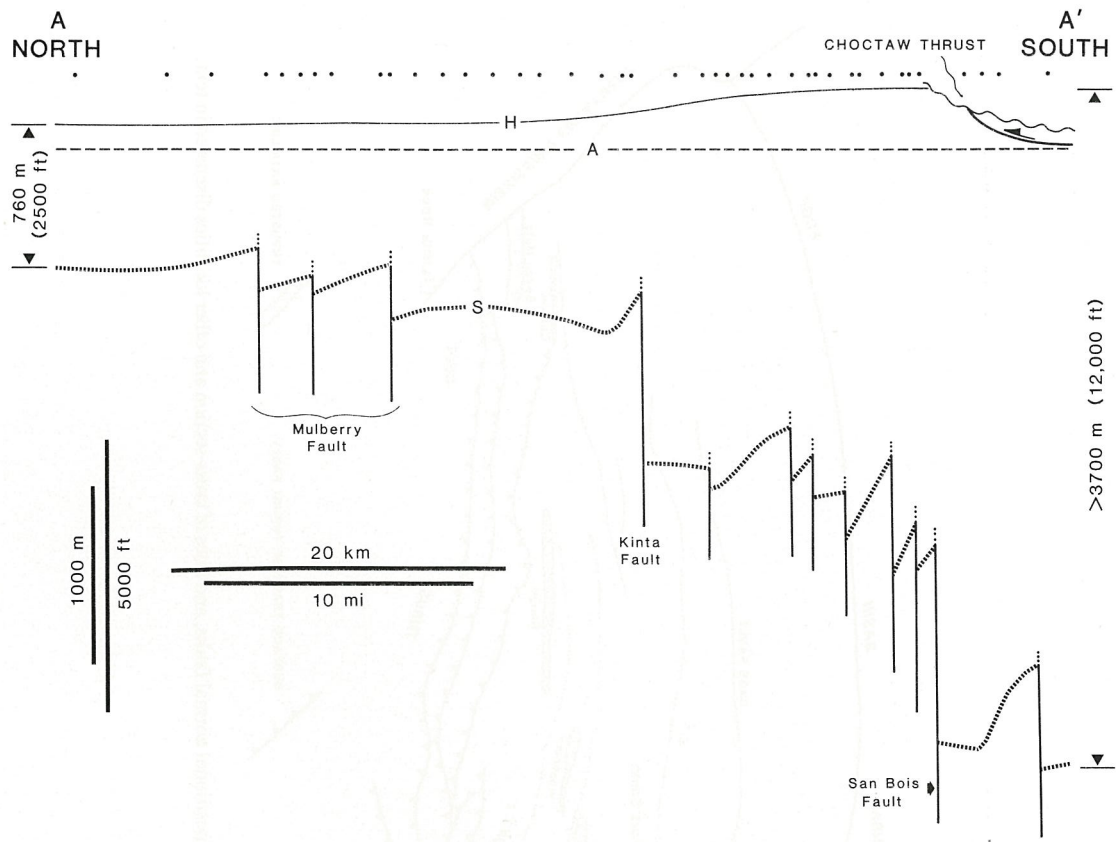

Fig. 6. Stratigraphic cross-section A–A′ constructed from wire-line logs from 41 wells, whose locations are indicated by black dots. S = Spiro sandstone, A = widespread upper Atoka key bed that serves as datum for cross-section, H = Hartshorne Sandstone.

Bois fault in cross-section B–B′ (Fig. 7) is only about 2400 m thick.

Southwards along the line of section, the Atoka thickens from less than 1200 m to more than 5500 m (estimated by projecting the horizon of the Hartshorne Sandstone), with syndepositional normal faults accounting for most of the increase. Moreover, the well at the south-eastern end of cross-section B–B′ did not penetrate the basal Atoka Spiro sandstone, suggesting that the estimate of 5500 m may be conservative. Alternatively, an undetected thrust fault may be present in the lower part of that well and bed E may be a subthrust equivalent of bed D (their log responses are similar); no other well has penetrated so deeply into the Atoka Formation and so this problem cannot be solved with available data. Nevertheless, the thickness of the Atoka section in the two south-easternmost wells approaches estimates of maximum Atoka thickness within the Ouachita frontal thrust belt, suggesting that the Atoka Formation in the frontal Ouachitas is simply the distal equivalent of the Atoka in the Arkoma basin and that both were deposited within a single basin.

There are an insufficient number of Spiro penetrations in this deep portion of the basin to analyse fault block geometry as was done for cross-section A–A′ and so the Spiro is schematically shown to have no apparent dip in Fig. 7. However, the extreme thickness of the Atoka Formation and the presence of several widespread key beds within the section provide an opportunity to discuss the relative timing of fault movement. It is apparent from the distribution of key beds (Fig. 7) that fault movement was not synchronous. Expansion of the section below bed D is limited to fault Y (and perhaps Z); expansion of the sections immediately below bed C and immediately below bed

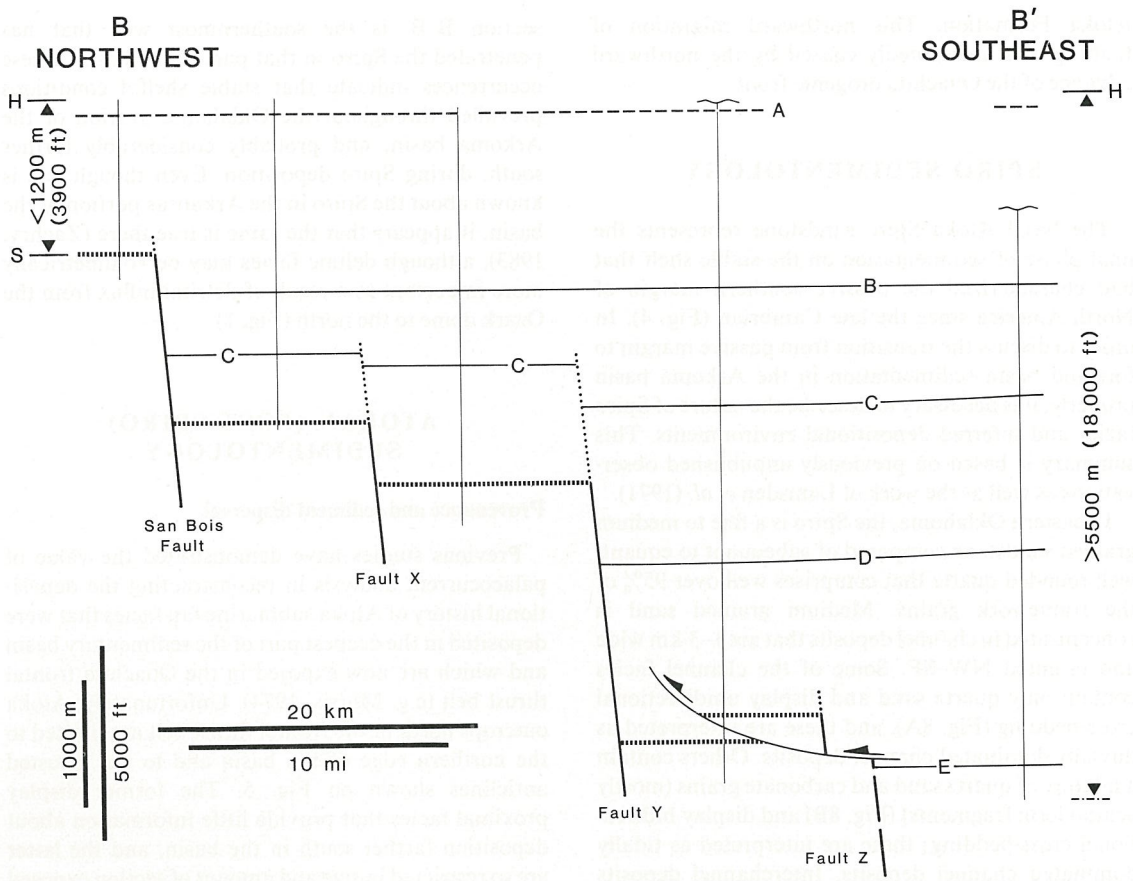

Fig. 7. Stratigraphic cross-section B–B′ constructed from wire-line logs from five wells, whose locations are indicated by vertical lines. Lines representing three wells on left extend from point of Hartshorne Sandstone penetration to total depth; lines representing two wells on right extend from present erosion surface (wavy lines) to total depth. S = Spiro sandstone; A = same bed labelled A in Fig. 6; B, C, D, and E = key beds within Atoka Formation; H = Hartshorne Sandstone. Bed A serves as datum for four wells on left; bed B serves as datum for well on right. Note thrust repeat of Spiro sandstone in fourth well from left.

B occurs across fault Y, fault X and the San Bois fault; expansion of the section immediately below bed A is limited to the San Bois fault. It appears that the southernmost syndepositional faults became active earliest and that active faulting migrated northwards with time. This general pattern is present throughout the basin.

One final aspect of syndepositional faulting merits description. Even though thickness increases in excess of 1000 m occur across many of these faults, there is absolutely no evidence of erosion of the Spiro sandstone or overlying strata on upthrown sides of the faults. There is typically a 100–200 m thick, dark grey shale immediately overlying the Spiro throughout the basin, and that shale is apparently the stratal equivalent of expanded sections downthrown to major faults.

To summarize, syndepositional normal faults fundamentally control the distribution and thickness of Atokan strata throughout the basin. Neither the basal Atoka Spiro sandstone nor the basal Demoinesian Hartshorne Sandstone displays evidence of syndepositional fault movement, thereby constraining normal faulting to an interval of time less than the duration of the Atokan age (approximately 5 Myr). Active normal faulting migrated northwards with time, resulting in a step-like onlap sequence within the

Atoka Formation. This northward migration of faulting was undoubtedly caused by the northward advance of the Ouachita orogenic front.

SPIRO SEDIMENTOLOGY

The basal Atoka Spiro sandstone represents the final phase of sedimentation on the stable shelf that had characterized the passive southern margin of North America since the late Cambrian (Fig. 4). In order to discuss the transition from passive margin to foreland basin sedimentation in the Arkoma basin properly, it is necessary to describe the nature of Spiro facies and inferred depositional environments. This summary is based on previously unpublished observations as well as the work of Lumsden *et al.* (1971).

In eastern Oklahoma, the Spiro is a fine to medium grained sandstone composed of subequant to equant, well rounded quartz that comprises well over 95% of the framework grains. Medium grained sand is concentrated in channel deposits that are 1–3 km wide and oriented NW–SE. Some of the channel facies contain only quartz sand and display unidirectional cross-bedding (Fig. 8A), and these are interpreted as fluvially dominated channel deposits. Others contain a mixture of quartz sand and carbonate grains (mostly echinoderm fragments) (Fig. 8B) and display bidirectional cross-bedding; these are interpreted as tidally dominated channel deposits. Interchannel deposits are composed of fine grained sand and shale organized into ripple bedded and thoroughly bioturbated sequences that were probably deposited in shallow subtidal through tidal flat environments (Fig. 8C, D). Overall, these characteristics suggest that rivers eroded sand from older, platform strata on the north side of the basin and delivered that sand to a broad, tidally swept, coastal environment. Full diameter cores from the southernmost part of the basin display similar sandstone facies as well as carbonate bank and interbank facies, indicating sedimentation on a marine shelf offshore from the tidal coastline.

As mentioned previously, the location of the original southern shelf edge is unknown. However, the southernmost known occurrences of Spiro coastal and shelfal facies are shown on Fig. 5. The open circle labelled C represents the location of an autochthonous (subthrust) cored interval and the one labelled C′ represents a palinspastically restored location of an allochthonous (thrust) cored interval in the same well; both display shoreline to shallow marine facies. Farther east, the circled location on the line of cross-section B–B′ is the southernmost well that has penetrated the Spiro in that part of the basin. These occurrences indicate that stable shelfal conditions prevailed throughout the Oklahoma portion of the Arkoma basin, and probably considerably farther south, during Spiro deposition. Even though less is known about the Spiro in the Arkansas portion of the basin, it appears that the same is true there (Zachry, 1983), although deltaic facies may be volumetrically more important as a result of detrital influx from the Ozark dome to the north (Fig. 1).

ATOKAN (POST-SPIRO) SEDIMENTOLOGY

Provenance and sediment dispersal

Previous studies have demonstrated the value of palaeocurrent analysis in reconstructing the depositional history of Atoka submarine fan facies that were deposited in the deepest part of the sedimentary basin and which are now exposed in the Ouachita frontal thrust belt (e.g. Morris, 1974). Unfortunately, Atoka outcrops north of the frontal thrust belt are limited to the northern edge of the basin and to the thrusted anticlines shown on Fig. 5. The former display proximal facies that provide little information about deposition farther south in the basin, and the latter are so restricted in size and amount of section exposed that they are of limited utility. Neither provides sufficient palaeocurrent data to allow reconstruction of sediment dispersal patterns within the basin proper. However, the petrology of Atoka sandstones can be used to interpret sediment dispersal patterns, at least on a gross scale.

Palaeotectonic and palaeographic reconstructions of the Arkoma basin and surrounding region (Graham *et al.*, 1975; Graham, Ingersoll & Dickinson, 1976; Houseknecht & Kacena, 1983; Thomas, 1985) suggest that the basin received sediment from three major dispersal systems during Atokan sedimentation. Detritus continued to be eroded from older platform strata to the north of the basin (Ozark dome and beyond) and sand derived from this continental provenance was predominantly composed of mature quartz grains like those deposited in the Spiro. Sediment was also funnelled southwards through the Illinois basin into the eastern Arkoma basin (Fig. 1), and sand associated with that dispersal system was also composed predominantly of quartz (Potter & Glass, 1958). The third dispersal system derived sediment from the Ouachita

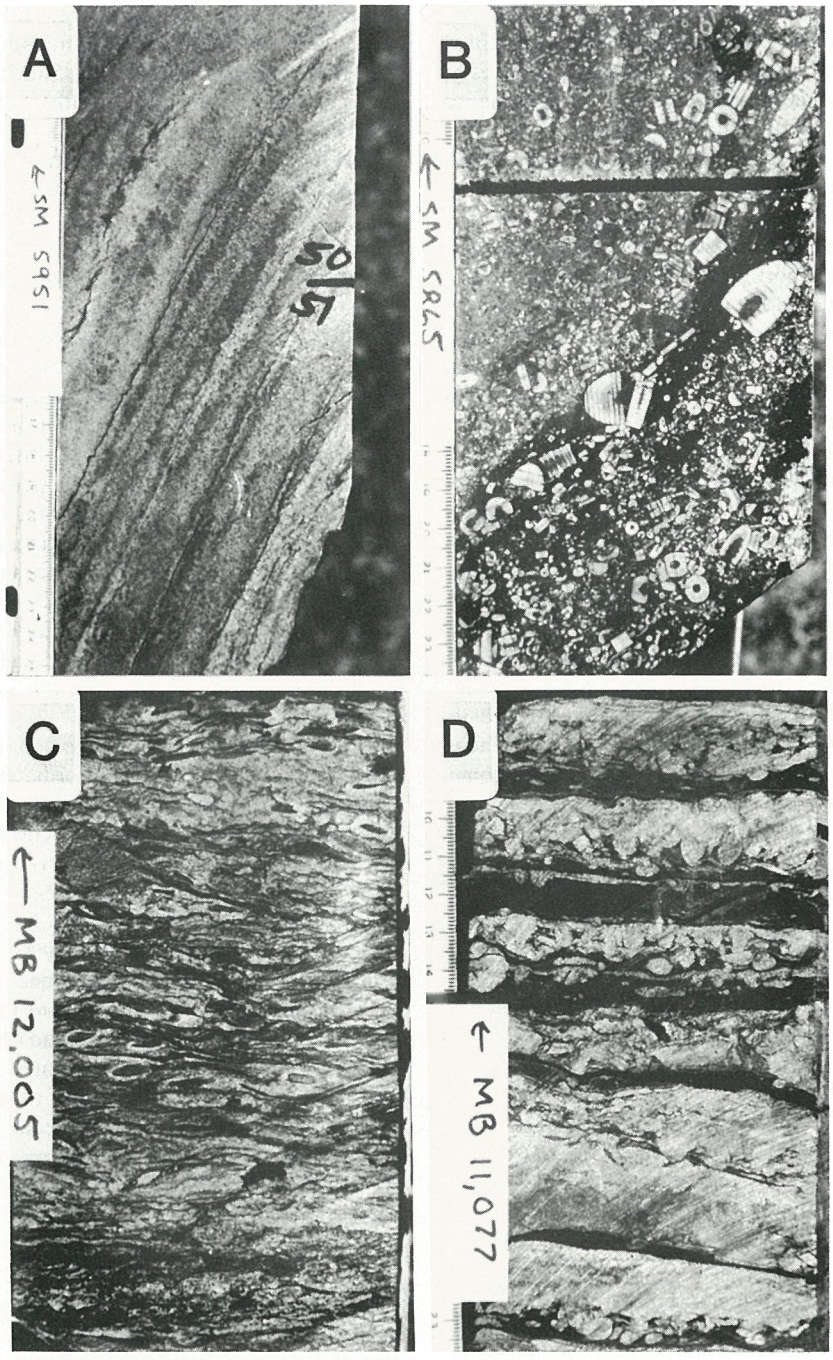

Fig. 8. Core photographs of facies in the Spiro sandstone. (A) Cross-bedded, quartzose sandstone of inferred fluvially dominated channel deposit (foreset dip is exaggerated by structural dip). (B) Cross-bedded, quartzose sandstone with abundant echinoderm fragments of inferred tidally dominated channel deposit (foreset dip is exaggerated by structural dip). (C) Thoroughly bioturbated interchannel facies. (D) Interbedded shale and bioturbated sandstone of interchannel facies. Ruler scales in centimetres; scale of (C) is the same as (D).

orogenic belt, which had already been uplifted and exposed to erosion along the south-western margin of the Black Warrior basin (Mack, Thomas & Horsey, 1983). Sand associated with that orogenic provenance contains a significant volume of lithic fragments and some feldspar, indicating derivation from metamorphic and volcanic source rocks (Mack *et al.*, 1983). Considerations of basin geometry (Figs 1, 4, 6 and 7) suggest that sand derived from the continental provenance to the north would have been transported more-or-less southwards into the basin and that sand derived from the other two areas would have entered the eastern portion of the basin and could only have reached other parts of the basin by westwards longitudinal transport.

Figure 9 summarizes framework grain composition of nearly 50 samples of Atoka (post-Spiro) sandstones collected in various parts of the basin. Those samples that plot within the field labelled Ozark petrofacies were collected at two locations indicated by triangles D and E in Fig. 5. Both the texture and composition of these samples are like the underlying Spiro and are consistent with derivation of sand from older platform strata north of the basin. The term 'Ozark petrofacies' is used to imply derivation from the north and to emphasize the widespread truncation of older Palaeozoic sandstones around the flanks of the Ozark dome as a likely source of this sand.

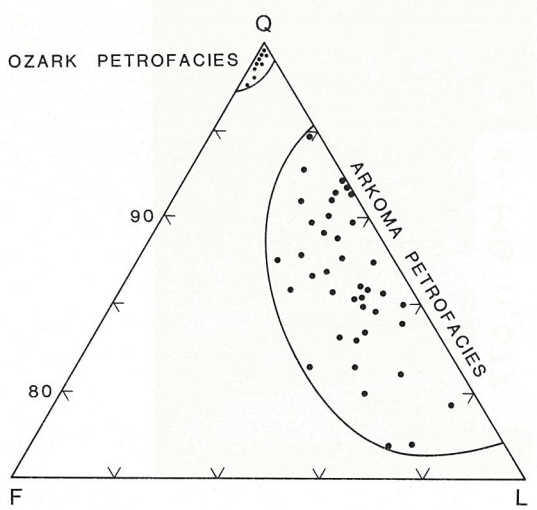

Fig. 9. QFL (quartz, feldspar, lithics) diagram showing framework grain composition of Ozark and Arkoma petrofacies. All lithic fragments are of metamorphic origin; feldspar is mostly albite. Composition is based on counting 300 points per sample.

Samples within the field labelled Arkoma petrofacies were collected from outcrops along all of the thrusted anticlines shown in Fig. 5 and from numerous wells in Oklahoma located south of the Milton and Backbone anticlines and north of the Ouachita frontal thrust belt. On a QFL diagram, these sandstones contain 75–90% quartz, and the quartz grains are very fine to fine grained, subelongate to subequant, and poorly to moderately rounded. Moreover, these sandstones contain 5–25% metamorphic lithic fragments (mostly slate and phyllite) and up to 8% feldspar (mostly albite). All of these characteristics significantly differ from those of the Ozark petrofacies and suggest derivation from an orogenic provenance, although the relatively quartzose samples within the Arkoma petrofacies may reflect a mixing of detritus from the orogenic source with either Ozark petrofacies or sand distributed through the Illinois basin. The framework grain composition of these sandstones is virtually identical to that of Atoka sandstones exposed in the Ouachita frontal thrust belt (Graham *et al.*, 1976; and unpublished data), suggesting a common provenance. The term 'Arkoma petrofacies' is used to emphasize the volumetric predominance of this sandstone composition within the basin.

In light of the foregoing discussion, it appears that most of the sand in the Atoka Formation was derived from the uplifted Ouachita orogenic belt to the east (SW of the Black Warrior basin), entered the eastern portion of the basin, and was transported longitudinally westwards to sites of deposition. Rapid subsidence associated with syndepositional normal faults undoubtedly promoted longitudinal dispersion of sediment. It is probably no coincidence that the Ozark petrofacies appears to be limited to that part of the basin north of the Mulberry fault and that the Arkoma petrofacies is pervasively distributed south of that fault (Fig. 5). Both its length and its position as the northernmost fault with significant displacement suggest that it may have exerted a major influence on the distribution of the two petrofacies.

Facies and environments of deposition

Synthesis of results from continuing research and previously published information allows reconstruction of the depositional system that prevailed during deposition of the Atoka Formation (for the sake of convenience, this discussion excludes the Spiro sandstone from the Atoka Formation). Figure 10 is a depositional model that illustrates relationships observed among Atoka facies and explains the influence

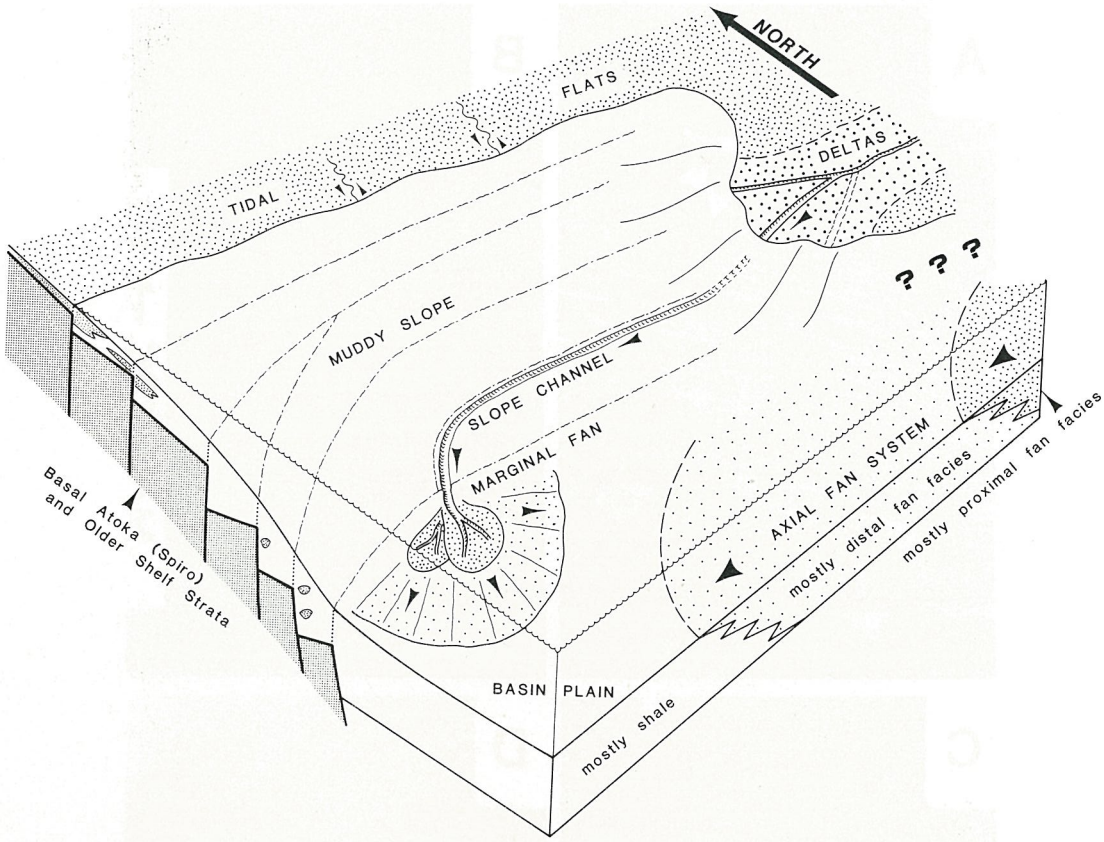

Fig. 10. Reconstruction of depositional system in which Atoka strata were deposited. Dash–dot lines represent the seafloor traces of syndepositional normal faults. The nature of the lateral relationship between deltaic facies and axial fan facies in the eastern portion of the basin is neither well documented nor well understood (as denoted by question marks), and should be considered schematic.

that syndepositional normal faulting exerted on sediment dispersal and the distribution of Atoka facies. The model is constrained by the fact that all facies illustrated are composed of Arkoma petrofacies and therefore must have been deposited within a system dominated by longitudinal sediment dispersal. It emphasizes sedimentation in that part of the basin where syndepositional faults were most active and where shallow to deep marine facies transitions occur over relatively short distances. It does not emphasize either fluvial-deltaic sedimentation along the northern margin of the basin (Zachry, 1983) or submarine fan sedimentation in the deepest part of the basin (Morris, 1974).

Shoreline facies

The northern limit of marine sedimentation in the Oklahoma portion of the basin is indicated by the presence of tidal flat shoreline facies (Fig. 10), whose southernmost extent occurs in the subsurface just south of the Milton and Backbone anticlines (Fig. 5). Marine shales grade upward via increasing number and thickness of sandstone beds into sand-dominated tidal flat facies, and the entire sequence displays a rich and diverse, shallow marine trace fossil assemblage (Chamberlain, 1978). The tidal flat facies comprise fining upward sequences like the one shown in Fig. 11(A), in which sand-flat, mixed-flat, and mud-flat subfacies are recognized. Sand-flat subfacies are composed of nearly 100% sand and display ripple-scale cross-bedding, swash bedding, and locally abundant U-shaped burrows (Fig. 11). Within the sand-flat subfacies, broadly channel-shaped beds displaying epsilon cross-bedding and siderite pebble lags probably represent deposition in meandering tidal channels. These sand-flat subfacies grade upward

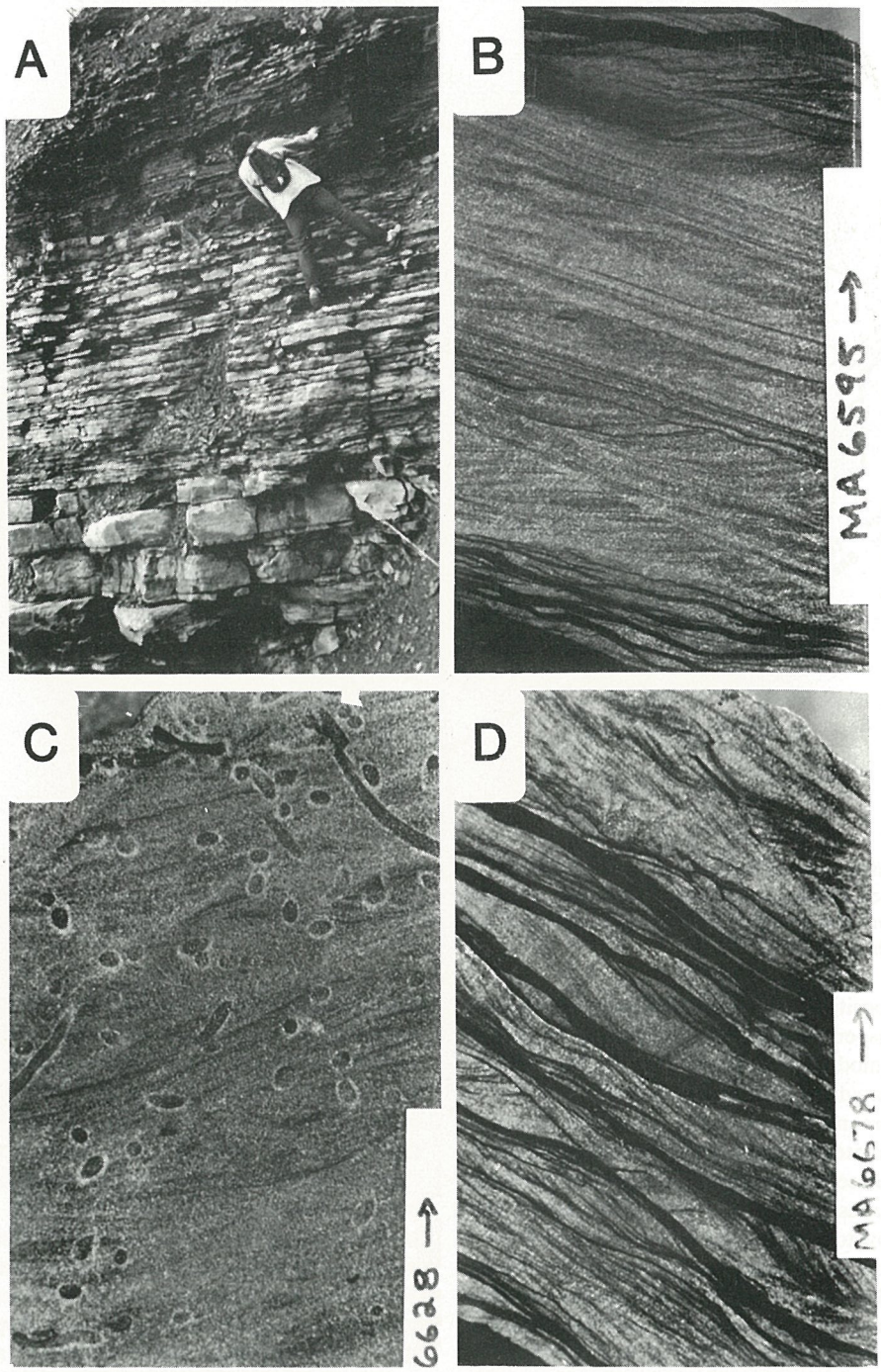

Fig. .. ...a tidal flat facies. (A) Outcrop view of fining upward sequence, showing upper part of sand-flat (bottom), mixed-flat (centre, at man's feet), and mud-flat (top, at man's head and hand) subfacies. (B) Core photograph of ripple-scale cross-bedding and swash bedding from sand-flat subfacies. (C) Ripple cross-bedded sand-flat subfacies displaying U-shaped burrows. (D) Ripple cross-bedded sandstone with shale interbeds from lower part of mixed-flat subfacies. Width of each core is 10 cm in (B), (C) and (D).

into mixed-flat subfacies that are composed of interbedded sandstone and shale (Fig. 11). The sandstone layers display ripple-scale cross-bedding, flaser bedding, and mud-draped, asymmetric ripples. With increasing mud content, the mixed-flat subfacies grade upward rather abruptly into mud-flat subfacies (Fig. 11A), which are composed mostly of silty mudstone. Individual, fining upward sequences are typically 5–8 m thick but vertical repetition of tidal flat sequences results in sand-rich, shoreline deposits that are locally more than 100 m thick.

Eastward in Arkansas, tidally dominated shoreline facies are exposed along all the anticlines shown in Fig. 5. These also display fining upward sequences that can be attributed to tidal flat sedimentation, but differ in that individual sequences range from 50 to 100 m in thickness and trace fossils are sparse. In every other detail, these facies are identical to those present in Oklahoma. Two factors are probably responsible for the presence of these overthickened sequences. First, they accumulated in that part of the basin most affected by syndepositional normal faulting and second, they were deposited closer to the location of major sediment input. Both the high rate of subsidence and the voluminous sediment influx would contribute to deposition of abnormally thick shoreline facies that contain sparse trace fauna.

Deltaic facies are also present in the Arkansas portion of the basin, although they are not as common as overthickened tidal flat facies. Marine shales grade upwards rather abruptly into sand-rich delta front subfacies, which display an abundance of ripple-scale cross-bedding and mud drapes. Locally such subfacies are interbedded with trough cross-bed sets that are typically about 50 cm thick. The latter probably represent deposition on distributary mouth bars by fluvial currents during high stage whereas the former represent tidal reworking of bar sediment during low stage. Delta front subfacies are typically overlain by distributary channel deposits, which display a predominance of trough cross-bedding and horizontal bedding. In those few outcrops where palaeocurrent data can be collected from distributrary channel subfacies, westwards palaeoflow is indicated. Atoka delta front and distributory channel deposits are virtually identical in both facies characteristics and indicated flow direction to Desmoinesian deltaic deposits of the basin described by Houseknecht *et al.* (1983). However, the limited distribution of Atoka deltaic facies relative to overthickened tidal flat facies suggests that tidal processes effectively reworked shoreline sediment and essentially destroyed many facies characteristics that are normally associated with deltaic sedimentation.

Slope facies

In the southern portion of the basin where the section thickens significantly across syndepositional faults, the Atoka comprises dark grey shale, which is unfossiliferous except for macerated and obviously transported plant debris, and numerous localized sandstones. Despite significant syndepositional displacement along many normal faults, numerous widespread key beds display continuity across the faults and there is absolutely no evidence of erosional truncation of strata upthrown to the faults (Figs 6 and 7). These relationships imply that the rate of mud deposition kept pace with the rate of subsidence and that the seafloor above the faults displayed little or no relief. However, it is equally apparent that these predominately pelitic facies grade southwards from shoreline facies discussed above into deep marine facies that are now exposed in the Ouachita frontal thrust belt. This combination of relationships suggests that deposition occurred on a gently dipping, muddy slope lacking a bathymetrically distinct shelf-slope-rise geometry (Fig. 10).

The localized sandstones that occur within these thick shales are difficult to analyse because they do not crop out anywhere around the basin and they are known primarily from wire-line log characteristics. Most of the sandstones that occur in this setting are lenticular (1–5 km wide; 10–50 m thick) and elongate (several kilometres to tens of kilometres long). Moreover, they are localized parallel and just downthrown to syndepositional normal faults. Fortunately, one such sandstone (the Red Oak) was extensively cored during its development as a major gas reservoir, and the preserved cores reveal much about deposition of sand on the muddy slope. The Red Oak, which is localized just below bed B and just downthrown to the San Bois fault in Fig. 7, is a multistoried sand body that has previously been interpreted as a submarine fan deposit (Vendros & Visher, 1978). In core, the base of each sandstone (story) is erosive, either into shale or a somewhat older sandstone bed. The sandstone is extremely uniform in grain size (very fine to fine sand) and sorting (moderately well to well sorted) and displays a limited range of sedimentary structures, with most cores appearing massive (Fig. 12). Other common structures include diffuse flat lamination and a diverse spectrum of dewatering structures, including dish structures, convolute lami-

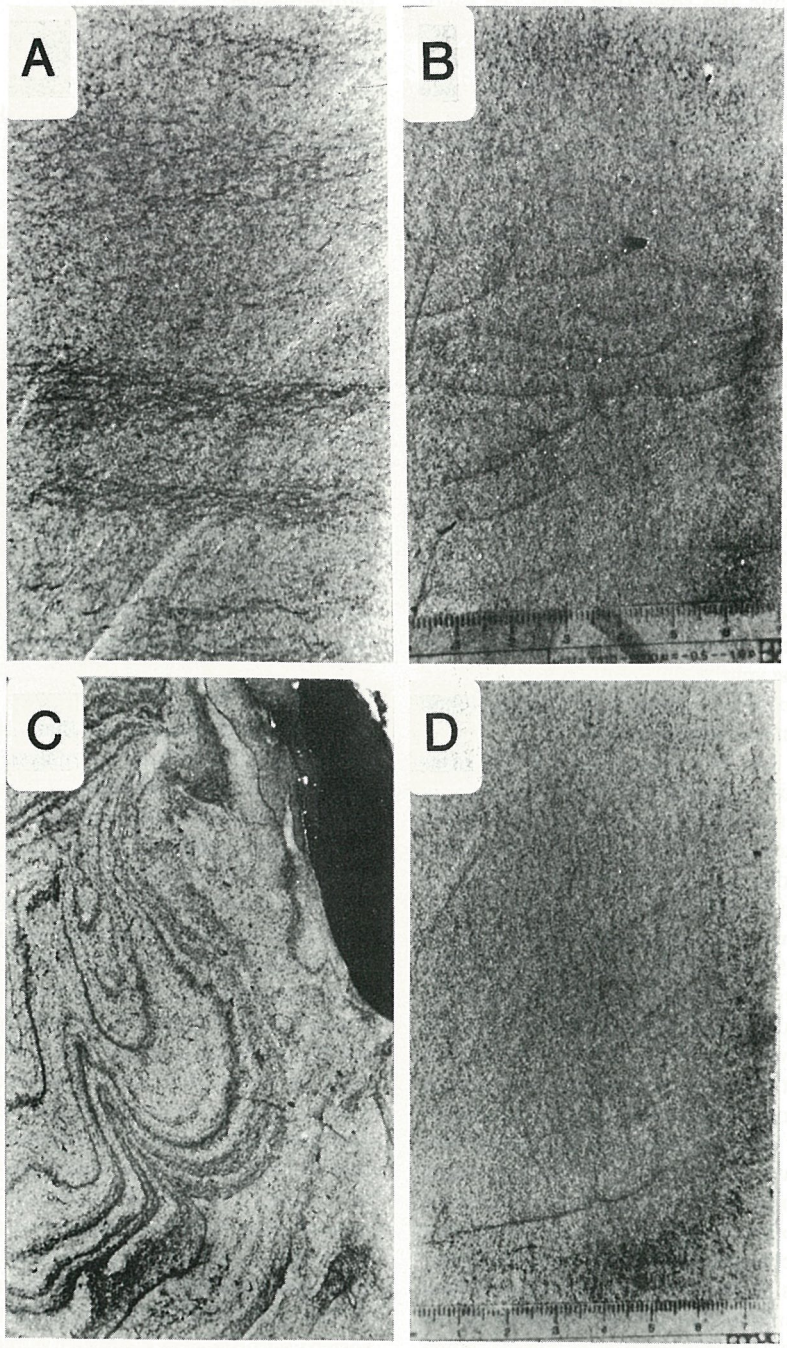

Fig. 12. Core photographs of sedimentary structures in the Red Oak sandstone. (A) Diffuse flat lamination overlain by massive sandstone. (B) Dish structures. (C) Convolute lamination. (D) Diffuse vertical lamination. Ruler scaled in centimetres in (B) and (D); (A) and (C) are the same scale.

nation, diffuse vertical lamination, swirled lamination, and dewatering pipes (Fig. 12) (Middleton & Hampton, 1976). Along the lateral margins of the lenticular sand bodies, silty sandstone displaying parallel lamination occurs, and identical facies are locally included as intraclasts within the sand body proper. There are no thin, widespread sandstone beds associated with these sand bodies, nor are there partial or complete Bouma sequences or any sort of graded beds present (over 350 m of core was described).

All of the characteristics enumerated above suggest deposition by channellized sediment gravity flows below storm wave base, with grain flow being the most likely specific process (Middleton & Hampton, 1976). It is proposed that deposition occurred in slope channels that were localized by rapid subsidence rates just downthrown to syndepositional normal faults (Fig. 10). Apparently the rotational sense of movement on certain faults (Fig. 6) resulted in at least a slight depression on the seafloor, which was sufficient to localize sediment gravity flows that entered the slope environment. The flows were erosive into unconsolidated slope muds, thereby channelizing the slope along the seafloor trace of syndepositional faults (Fig. 10). It appears that levee facies were locally deposited along the margins of the slope channels (parallel bedded silty sandstones), but there is no evidence of deposition by unconfined sediment gravity flows as would be expected on submarine fan lobes.

Atoka sandstones like the Red Oak have long been attributed to deposition in 'deep water' because of the predominance of sedimentary structures indicative of sediment gravity flow mechanisms. As a result, many previous workers have inferred that the syndepositional normal faults acted as fundamental bathymetric features within the depositional basin, with shelfal conditions prevailing upthrown and 'deep water' conditions prevailing downthrown to a major fault (e.g. Vedros & Visher, 1978). This inference does not seem compatible with the continuity of correlative beds across many syndepositional faults (Fig. 7) and needs to be re-evaluated in the light of voluminous recent work demonstrating that the only requisite for accumulation and preservation of facies deposited by sediment gravity flow mechanisms is water depths below storm wave base (e.g. Walker, 1979). Within a tidally dominated basin like the Arkoma, it is feasible for such deposits to accumulate in water depths that would not normally be considered 'deep'. In support of this interpretation, the tidal flat facies illustrated in Fig. 11 (B–D) occur in a sandstone that is only 200 m up section from the Red Oak sandstone illustrated in Fig. 12, and both sandstones occur at the same location in the basin. Assuming that neither uplift of the basin nor a significant drop in sea-level occurred after deposition of the slope channel facies and before deposition of the tidal flat facies (neither of which is likely), 200 m is a reasonable estimate for the depth of water in which the Red Oak slope channel sand was deposited.

Submarine fan facies

As mentioned previously, numerous workers have published details of submarine fan facies that were deposited on the deep basin floor and are now exposed in the Ouachita frontal thrust belt. These are illustrated schematically and labelled 'axial fan system' in Fig. 10. However, there are also smaller submarine fan sequences that were apparently deposited at the toe of the slope as distal facies equivalents of slope channels discussed above, and these are labelled 'marginal fan' in Fig. 10. In outcrops along the frontal thrust belt, these facies can be distinguished from those associated with the axial fan system in three ways. First, the marginal fans are composed of 'cleaner' sandstone than the axial fans. Petrographic analysis reveals that the framework grain composition of sandstones in the two facies are identical, but samples of the axial fan system contain significantly more matrix and are more poorly sorted than samples of the marginal fan system. Second, deposits associated with the axial fan system invariably display westward directed palaeocurrent indicators whereas marginal fan facies display southwards to south-westwards indicators. Thirdly, the marginal fan deposits display internal facies architecture that suggests progradation from north to south. For example, channellized proximal lobe facies grade both westwards and eastwards along the strike of the frontal thrust belt into more distal lobe facies characterized by beds deposited by unconfined sediment gravity flows. The dimensions of such lateral facies sequences are typically 15–25 km, suggesting the original size of the marginal fans. As indicated in Fig. 10, there is abundant evidence for interfingering of marginal and axial fan facies, suggesting that the two systems evolved simultaneously but were fed by different sediment dispersal systems.

SUMMARY

The Arkoma foreland basin developed in response to convergent tectonism associated with the Ouachita

orogenic event. During Atokan time, the tectonically stable shelf that had characterized the passive margin of southern North America was broken down by normal faults induced by obduction of the Ouachita accretionary prism on to the continental crust. The lower and middle portion of the Atoka Formation comprises a wedge of strata that displays thickness, petrofacies, and depositional facies patterns that were significantly influenced by syndepositional movement along these normal faults. By the end of Atokan time, fault movement had ceased and the basin was characterized by flexural subsidence induced by foreland-style thrust loading and shallow marine through non-marine sedimentation in a fully formed foreland basin.

ACKNOWLEDGMENTS

This work has benefited tremendously from interaction with, and funding from Tenneco Oil Company; I particularly appreciate the input of Mac McGilvery, Mike Albano, and W. D. Hollar. Significant contributions have been made by former students E. C. Williams and S. N. Williams. The project has also been supported with funding and/or data provided by ARCO, Marathon, Sampson Resources, Santa Fe Minerals, Sohio, and Texaco.

REFERENCES

BERRY, R.M. & TRUMBLY, W.D. (1968) Wilburton gas field, Arkoma basin, Oklahoma. In: *Geology of the Western Arkoma Basin and Ouachita Mountains* (Ed. by L. M. Cline), pp. 86–103. *Okla. City geol. Soc. Guidebook.*

BUCHANAN, R.S. & JOHNSON, F.K. (1968) Bonanza gas field—a model for Arkoma basin growth faulting. In: *Geology of the Western Arkoma Basin and Ouachita Mountains* (Ed. by L.M. Cline), pp. 75–85. *Okla. City geol. Soc. Guidebook.*

CHAMBERLAIN, C.K. (1978) *Trace fossils and paleoecology of the Ouachita geosyncline. Soc. econ. Paleont. Miner. Guidebook*, 68 pp.

DICKINSON, W.R. (1974) Plate tectonics and sedimentation. In: *Tectonics and Sedimentation* (Ed. by W. R. Dickinson). *Spec. Publ. Soc. econ. Paleont. Miner., Tulsa*, **22**, 1–27.

DICKINSON, W.R. (1976) Plate tectonics and hydrocarbon accumulations. *Am. Ass. Petrol. Geol. Short Course 1.*

FLAWN, P.T., GOLDSTEIN, A. Jr, KING, P.B. & WEAVER, C.E. (1961) The Ouachita System. *Bur. econ. Geol., Univ. Texas Pub 6120*, 401 pp.

GRAHAM, S.A., DICKINSON, W.R. & INGERSOLL, R.V. (1975) Himalayan–Bengal model for flysch dispersal in the Appalachian–Ouachita system. *Bull. geol. Soc. Am.* **86**, 273–286.

GRAHAM, S.A., INGERSOLL, R.V. & DICKINSON, W.R. (1976) Common provenance for lithic grains in Carboniferous sandstones from Ouachita Mountains and Black Warrior basin. *J. sedim. Petrol.* **46**, 620–632.

HALEY, B.R. (1982) Geology and energy resources of the Arkoma basin, Oklahoma and Arkansas. *Univ. Mo.-Rolla J.* **3**, 43–53.

HOUSEKNECHT, D.W., ZAENGLE, J.F., STEYAERT, D.J., MATTEO, A.P. Jr & KUHN, M.A. (1983) Facies and depositional environments of the Desmoinesian Hartshorne Sandstone, Arkoma basin. In: *Tectonic–Sedimentary Evolution of the Arkoma Basin* (Ed. by D. W. Houseknecht). *Soc. econ. Paleont. Miner. Midcont. Sec.* **1**, 53–82.

HOUSEKNECHT, D.W. & KACENA, J.A. (1983) Tectonic and sedimentary evolution of the Arkoma foreland basin. In: *Tectonic–Sedimentary Evolution of the Arkoma Basin* (Ed. by D. W. Houseknecht). *Soc. econ. Paleont. Miner. Midcont. Sec.* **1**, 3–33.

HOUSEKNECHT, D.W. & MATTHEWS, S.M. (1985) Thermal maturity of Carboniferous strata, Ouachita Mountains. *Bull. Am. Ass. Petrol. Geol.* **69**, 335–345.

JORDAN, T.E. (1981) Thrust loads and foreland basin evolution, Cretaceous, western United States. *Bull. Am. Ass. Petrol. Geol.* **65**, 2506–2520.

KOINM, D.N. & DICKEY, P.A. (1967) Growth faulting in McAlester basin of Oklahoma. *Bull. Am. Ass. Petrol. Geol.* **51**, 710–718.

LILLIE, R.J., NELSON, K.D., DE VOOGD, B., BREWER, J.A., OLIVER, J.E., BROWN, L.D., KAUFMAN, S. & VIELE, G.W. (1983) Crustal structure of Ouachita Mountains, Arkansas: a model based on integration of COCORP reflection profiles and regional geophysical data. *Bull. Am. Ass. Petrol. Geol.* **67**, 907–931.

LUMSDEN, D.N., PITTMAN, E.D. & BUCHANAN, R.S. (1971) Sedimentation and petrology of Spiro and Foster sands (Pennsylvanian), McAlester basin, Oklahoma. *Bull. Am. Ass. Petrol. Geol.* **55**, 254–266.

MACK, G.H., THOMAS, W.A. & HORSEY, C.A. (1983) Composition of Carboniferous sandstones and tectonic framework of southern Appalachian–Ouachita orogen. *J. sedim. Petrol.* **53**, 931–946.

MIDDLETON, G. & HAMPTON, M. (1976) Subaqueous sediment transport and deposition by sediment gravity flows. In: *Marine Sediment Transport and Environmental Management* (Ed. by D. Stanley and D. Swift), pp. 197–218. Wiley, New York.

MOIOLA, R.J. & SHANMUGAM, G. (1984) Submarine fan sedimentation, Ouachita Mountains, Arkansas and Oklahoma. *Trans. Gulf-Cst Ass. geol. Soc.* **34**, 175–182.

MORRIS, R.C. (1974) Sedimentary and tectonic history of the Ouachita Mountains. In: *Tectonics and Sedimentation* (Ed. by W. R. Dickinson). *Spec. Publ. Soc. econ. Paleont. Miner., Tulsa.*, **22**, 120–142.

NICHOLAS, R.L. & WADDELL, D.E. (1982) New Paleozoic subsurface data from the north-central Gulf Coast (abstract). *Abstr. Prog. geol. Soc. Am.* **14**, 576.

POTTER, P.E. & GLASS, H.D. (1958) Petrology and sedimentation of the Pennsylvanian sediments in southern Illinois—a vertical profile. *Ill. geol. Surv. R.I.* **204**, 60 pp.

THOMAS, W.A. (1977) Evolution of Appalachian-Ouachita salients and recesses for reentrants and promontories in the continental margin. *Am. J. Sci.* **277**, 1233–1278.

THOMAS, W.A. (1985) The Appalachian–Ouachita connection: Paleozoic orogenic belt at the southern margin of North America. *Ann Rev. Earth planet. Sci.* **13**, 175–199.

VEDROS, S.G. & VISHER, G.S. (1978) The Red Oak sandstone: a hydrocarbon-producing submarine fan deposit. In: *Sedimentation in Submarine Canyons, Fans, and Trenches* (Ed. by D. J. Stanley & G. Kelling), pp. 292–308. Dowden, Hutchinson & Ross, Stroudsburg.

WALKER, R. G. (1979) Shallow marine sands. In: *Facies Models* (Ed. by R. G. Walker). *Geosc. Can. Reprint Ser.* **1**, 75–89.

ZACHRY, D.L. (1983) Sedimentologic framework of the Atoka Formation, Arkoma basin, Arkansas. In: *Tectonic–Sedimentary Evolution of the Arkoma Basin* (Ed. by D. W. Houseknecht). *Soc. econ. Paleont. Miner. Midcont. Sec.* **1**, 34–52.